The Cost of Seven-brane Gauge Symmetry in a Quadrillion F-theory Compactifications

James Halverson and Jiahua Tian

Department of Physics, Northeastern University, Boston, MA 02115-5000 USA

We study seven-branes in $O(10^{15})$ four-dimensional F-theory compactifications where seven-brane moduli must be tuned in order to achieve non-abelian gauge symmetry. The associated compact spaces B are the set of all smooth weak Fano toric threefolds. By a study of fine star regular triangulations of three dimensional reflexive polytopes, the number of such spaces is estimated to be $5.8\times10^{14} \lesssim N_{\text{bases}} \lesssim 1.8\times10^{17}$. Typically hundreds or thousands of moduli must be tuned to achieve symmetry for $h^{11}(B) < 10$, but the average number drops sharply into the range $O(25)$-$O(200)$ as $h^{11}(B)$ increases. For some low rank groups, such as $SU(2)$ and $SU(3)$, there exist examples where only a few moduli must be tuned in order to achieve seven-brane gauge symmetry.

arXiv:1610.08864v1 [hep-th] 27 Oct 2016

1. Introduction.

Non-abelian gauge theories play a central role in particle physics, and a celebrated question in string theory is whether such sectors should be expected. One might think the answer is obvious, since they are implicit in certain ten-dimensional superstring theories, but those symmetries can be broken by compactification and restored only at special subloci in the associated moduli space. Whether such enhanced symmetry loci exist, the physics that stabilizes vacua on them, and the dynamics that might drive the universe to those vacua are all relevant cosmological questions in the string landscape; see e.g. [1, 2] and references therein.

F-theory [3] is a generalization of the type IIb superstring that allows the axiodilaton to vary in the extra spatial dimensions. It provides a broad view of the landscape: in weakly coupled type IIb limits [4, 5] it realizes the best understood moduli stabilization scenarios [6, 7], strong coupling effects are computable by the power of holomorphy realized in complex algebraic geometry [3, 8], and many landscape studies have been performed in this context, see e.g. [9–12].

Non-abelian gauge sectors may arise on seven-branes in F-theory, the structure of which may be encoded in the geometry of a Calabi-Yau elliptic fibration $X \xrightarrow{\pi} B$, where B is the compact extra dimensional space. In this paper we will focus on four-dimensional compactifications, in which case B is an algebraic threefold. The seven-branes wrap a four-dimensional space $\Delta = 0$ in B that may have many components, giving rise to many intersecting seven-branes. Each seven-brane may carry an associated non-abelian gauge factor G that is determined in part by Kodaira's classification [13–15] of singular fibers, as well as additional geometric data [16] in B, T-branes [17], and G-flux [18]. All are important, but the geometrically determined data provides a foundation for the seven-brane physics and is necessary for the existence of non-abelian gauge symmetry, and therefore we focus on it here. The associated gauge group is more accurately called the geometric gauge group, but for brevity we will drop such a distinction and refer to the gauge group of a seven-brane. The gauge group of a seven-brane is determined by the structure of X, but if the complex structure of X is varied in the complex structure moduli space $\mathcal{M}_{cs}(X)$, then the seven-branes may be deformed and the gauge symmetry may be broken. The question of the existence of loci with non-abelian gauge symmetry may then be studied in the context of $\mathcal{M}_{cs}(X)$, which depends critically on the topology of B.

Recently there has been much work on so-called non-Higgsable clusters, which are seven-brane gauge sectors that exist for generic points in $\mathcal{M}_{cs}(X)$, and their properties are determined by B. These structures do not exist in eight dimensional compactifications, but do in six [8, 19–22] and four [2, 23–26] dimensional compactifications. Gauge factors that may appear on a seven-brane in such a cluster include

$$G \in \{E_8, E_7, E_6, F_4, SO(8), SO(7), G_2, SU(3), SU(2)\} \tag{1}$$

and the possible Lagrangian two-factor gauge sectors on adjacent seven-branes in such a cluster are

$$\begin{aligned} G_1 \times G_2 \in \{&SU(3)\times SU(3), G_2 \times SU(2),\\ &SO(7)\times SU(2), SU(3)\times SU(2),\\ &SU(2)\times SU(2)\}. \end{aligned} \tag{2}$$

Note that $SU(3)$ and $SU(2)$ are the allowed $SU(N)$ groups, whereas $SU(5)$ and $SO(10)$ never occur for generic moduli [2]. Non-Higgsable clusters in four-dimensional compactifications may have interesting topologies [24], motivate phenomenological models [2, 25–27], and have implications for symmetry in the landscape [2]. The latter is strengthened by analytical arguments and growing evidence [20, 23, 25, 26] that nearly all known extra dimensional spaces B give rise to non-Higgsable clusters.

Conversely, some spaces B do not exhibit seven-brane gauge symmetry at generic points in $\mathcal{M}_{cs}(X)$. Seven-brane gauge symmetry often exists on subloci in $\mathcal{M}_{cs}(X)$, though, in which case arriving in such a vacuum requires that those vacua are stabilized and cosmologically populated. While at this point it is difficult to address issues of

dynamics, recent estimates [28, 29] show that the number of flux vacua on subloci with symmetry is exponentially suppressed relative to the number without symmetry (i.e. at generic points in $\mathcal{M}_{cs}(X)$). For example, there exist B where flux vacua with $SU(5)$ gauge group are suppressed [28] by a factor of $e^{O(1000)}$ relative to those with no gauge symmetry. These suppression factors get larger as the codimension in $\mathcal{M}_{cs}(X)$ necessary to obtain gauge symmetry grows.

In this paper we study seven-brane gauge symmetry in a quadrillion, i.e. $O(10^{15})$, four-dimensional F-theory compactifications that do not exhibit gauge symmetry at generic points of $\mathcal{M}_{cs}(X)$. The results of [28] extrapolated to these compactifications would imply that, for fixed B, the number of flux vacua with symmetry is exponentially suppressed relative to the number of flux vacua without symmetry. Rather than computing numbers of flux vacua, we will instead measure the "cost" of symmetry by computing the number of moduli that must be tuned to engineer seven-brane gauge symmetry on any toric divisor in any smooth weak Fano toric threefold, which are in one to one correspondence with fine star regular triangulations of the 4319 reflexive polytopes [30]; a variety is weak Fano if $-K \cdot C > 0$ for all holomorphic curves C, where $-K$ is an anticanonical divisor. We will do this for gauge groups in the set

$$\begin{aligned} G \in \{&SU(2), SU(3), SU(4), SU(5), \\ &SO(7), Sp(1), Sp(2), SO(8), \\ &SO(9), SO(10), G_2, F_4, E_6, E_7, E_8\}, \end{aligned} \tag{3}$$

some of which may arise in a number of ways.

If non-Higgsable clusters are a solution to a tuning (in moduli) problem in the landscape, one goal of this paper is to diagnose the severity of the problem by studying models that do not exhibit non-Higgsable clusters. Compared to the results of [28], the larger set of spaces B that we study suggests that the problem may be less severe. Specifically, spaces B in this set with $h^{11}(B) < 10$, which contain those of [28], require tuning hundreds or thousands or moduli in $\mathcal{M}_{cs}(X)$, but this number drops sharply into the range $O(20)$-$O(250)$ for $h^{11}(B) > 20$. It is reasonable to expect that the associated suppressions in ratios of flux vacua are much smaller than e^{1000}, though likely still quite large. We leave vacuum statistics to future work. We have also found examples where tuning a low rank group G on a seven-brane on particular divisors D requires turning off only a few moduli; this is far from generic, but interesting nonetheless.

This paper is organized as follows. In Section 2 we study fine-regular-star triangulations (FRST) of $3d$ reflexive polytopes, which is important for statistical weighting of spaces B. In Section 3 we study the cost of tuning gauge symmetry on various types on seven-branes wrapped on all toric divisors in all smooth weak Fano toric threefolds. In Section 4 we will conclude.

2. Landscape Estimates and Weights

In this section we compute or estimate the number of fine-regular-star triangulations (FRST) of each of the 4319 $3d$ reflexive polytopes [30]. These are in one-to-one correspondence with smooth weak Fano toric threefolds, which serve as the extra dimensional spaces B of the F-theory compactifications that we study.

Though the toric varieties associated to different FRST of the same polytope have the same tuning costs, the number of FRST per polytope must be taken into account in computing a weighted average of the cost of symmetry across all 4319 polytopes. We will compute or estimate the number of bases for each values of $h^{11}(B)$, which ranges from 1 to 35.[1] The details are described in the following two subsections.

Approximate Number of FRST

The number of FRST increases rapidly with $h^{11}(B)$, necessitating different approximations for the number of FRST of a given polytope as $h^{11}(B)$ increases. These methods will be called A, B, C, D, and we will describe them in detail in this section. Throughout, we the number of lattice points in P, including the origin, as n_P. Hence, the corresponding toric variety has $h^{11}(B) = n_P - 4$ and $n_P - 1$ toric divisors.

Method A is to perform the exact calculation of the number of FRST. Specifically, we compute the exact numbers of FRST of the 1943 polytopes that have $n_P \leq 14$, which corresponds to $h^{11}(B) \leq 10$. Computing all FRST for $h^{11}(B) = 10$ takes multiple days of computer time, motivating the use of approximation methods.

Method B is our most accurate approximation method: when $11 \leq h^{11}(B) \leq 22$ we approximate the number of FRST of a polytope P by the product of the fine-and-regular triangulations (FRT) of each of its facets. This approximation is justified by two facts: 1) This method computes an estimated number of FRST within 10% of the exact values for $h^{11}(B) \leq 10$, as shown in Figure 1; 2) Only the order of magnitude of number of FRST matters for our purposes, since this number can reach the order $10^9 - 10^{17}$ when $h^{11}(B) \geq 30$, and therefore a small error won't qualitatively change the results.

The results of method B for $h^{11}(B) \leq 22$ is shown in Figure 2. Although we have computed the exact numbers of FRST for $h^{11}(B) \leq 10$, the same estimate is also calculated for those cases so that we can see an approximately linear behavior of $\log_{10} N_T$ as a function of $h^{11}(B)$ when $7 \leq h^{11}(B) \leq 22$.

We find that method B is very time-consuming when applied to a polytope with $n_P \geq 27$, which corresponds to $h^{11}(B) \geq 23$. There are 91 polytopes with this property.

[1] Note that there is no base space with $h^{11}(B) = 33$ or 34.

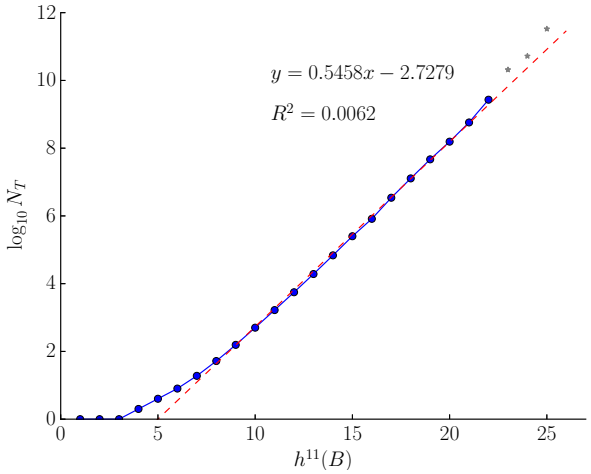

FIG. 1: The logarithm of the average numbers of triangulations N_T per polytope when using different methods for $h^{11}_B \leq 10$. The red curve denotes the exact result, i.e. method A, whereas the blue curve estimates the number of FRST using method B.

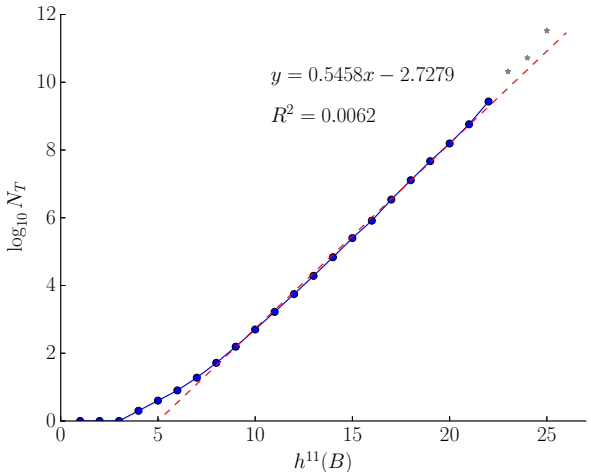

FIG. 2: The logarithm of the average number of triangulations N_T using method B. A line fits the data to high accuracy for $7 \leq h^{11}(B) \leq 22$. The grey stars shows on the plot are explained in the description of method C.

Method B breaks down for those 91 polytopes since triangulating the individual facets becomes too costly. That usually happens when the polytope contains a facet with $n_F \geq 19$ where n_F is the number of lattice points on the facet.

To find a method to accurately estimate the number of FRT of such facets, we use the results of [31] where the authors employed recursions that allows one to compute the number of triangulations for certain rectangular areas using dynamic programming. This allows us to obtain lower and upper bounds for the number of FRT of that facet, and then multiply with the exact numbers of FRT of the other facets to give an approximation to the number of FRST of the polytope. The calculation of these bounds on the number of FRT is highly dependent on the shape of the facet.

We first focus on the 38 polytopes for which $n_P \geq 30$ ($h^{11}(B) \geq 26$). This relatively small set can be investigated case by case. The 8 polytopes shown in Table I are those with $n_P \geq 30$ that have no facet[2] with $n_F > 19$. Therefore the estimate can be done using method B.

P	$h^{11}(B)$	Number of FRST	P	$h^{11}(B)$	Number of FRST
2	31	3.034×10^{15}	4	26	1.275×10^{12}
128	26	3.860×10^{12}	130	27	1.174×10^{13}
134	26	1.809×10^{12}	136	26	2.773×10^{12}
296	26	2.399×10^{11}	780	26	1.508×10^{12}

TABLE I: These are the products of the numbers of FRST on each facet of the polytope. The polytope index is given by *Sage 7.2* using `PALPreader`, indexing from one.

For $n_P \geq 30$ polytopes with a facet of $n_F \geq 19$ we compute the bounds on the number of FRT triangulations. The computation depends on the shape of such facets, which can be classified into 6 types as shown by the shaded areas in Figure 3. The unshaded area is added to make the shape be rectangular so that the results in [31] can be applied, as described previously. The number of fine triangulations (FT) of these rectangular areas are exactly calculated in [31] and at least 70% of them are FRT; This will suffice since again we are concerned with obtaining the correct order of magnitude. The lower bound of the numbers of FT of the shaded area, denoted N_S, is determined by using the method of [31] to calculate the numbers of FT of the strips of points in this region, and then taking the product of them since gluing two fine-triangulated 2d point sets along a common edge gives a FT of their union. The upper bound is computed using the fact that $N_S \times N_{US} \leq N_R$, where N_{US} is the number of FT of the unshaded area and N_R is that of the total rectangular area. Let κ be the lower bound on N_{US} computed by the same method as for computing

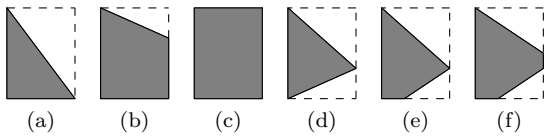

FIG. 3: Shapes of facets

[2] Actually there is a facet in polytope 296 with $n_F = 19$, and this is the only case that the calculation can be done in a reasonable time. Since the others take too long to compute, we will just give the estimates for them.

the lower bound of N_S. Then $N_S \leq N_R/N_{US} \leq N_R/\kappa$ gives an upper bound on N_S. We present the bounds on the number of FT of large facets of all polytopes with $n_P \geq 30$ in Table II, and the associated bounds on the number of FRST of those polytopes in Table III. This is the approximation method we refer to as method D.

P	Case	Lower bound	Upper bound
8	a	6.112×10^7	4.471×10^{10}
10	a	9.459×10^6	2.415×10^9
12	a	6.236×10^7	3.919×10^{10}
18	a	4.204×10^5	6.434×10^7
74	b	2.037×10^6	1.550×10^8
80	a	1.323×10^5	1.614×10^7
88	b	8.732×10^5	2.080×10^9
90	b	6.306×10^5	4.099×10^9
100	e	6.418×10^6	7.026×10^{11}
223	d	3.209×10^7	2.616×10^{11}
236	a	1.323×10^5	1.614×10^7
256	c	7.370×10^8	
260	b	2.037×10^7	8.318×10^9
266	b	1.323×10^5	1.990×10^8
270	c	7.370×10^8	
272	b	9.459×10^6	7.307×10^9
293	d	4.204×10^5	3.666×10^9
348	b	9.460×10^6	7.307×10^9
352	b	6.306×10^5	4.657×10^7
387	b	1.715×10^6	1.842×10^8
521	a	4.204×10^5	6.434×10^7
527	e	6.306×10^5	6.200×10^9
553	b	6.305×10^5	2.990×10^9
762	b	1.774×10^5	4.657×10^7
798	b	1.323×10^5	1.990×10^8
810	c	7.370×10^8	
812	b	2.037×10^6	1.550×10^8
840	f	8.732×10^5	2.721×10^8
985	d	3.153×10^6	7.131×10^9
1000	b	1.774×10^5	2.666×10^8

TABLE II: Estimates of the number of FT for a facet

For $23 \leq h^{11}(B) \leq 25$ the situation is more difficult, since application of method B is generally time consuming and there are too many polytopes to do a case by case analysis of bounds. For some polytopes where there is no facet with $n_F \geq 19$ it is possible to apply method B. Figure 2 depicts the average FRST estimates for these polytopes obtained using method B, where the averages are labelled by grey stars; note that they lie close to the linear fit line. For these reasons we believe it is justified to take the average values of those cases as an approximation to the numbers of FRST for polytopes with $23 \leq h^{11}(B) \leq 25$; this is method C.

Estimate of the number of base spaces

In this subsection we estimate the number of base spaces that we consider, which is equivalent to the number of FRST of $3d$ reflexive polytopes. In order to get a more accurate estimate we take into account the effect of fan isomorphisms induced by lattice isomorphisms, which relate identical toric bases B. Since there are no lattice isomorphisms between different polytopes, the associated fans cannot be isomorphic to each other, and therefore only the fan automorphisms within a polytope need to be considered.

P	h_{11}	Lower bound	Upper bound
8	35	2.320×10^{14}	1.697×10^{17}
10	31	5.710×10^{12}	1.458×10^{15}
12	35	7.715×10^{13}	4.849×10^{16}
18	26	2.899×10^9	4.436×10^{11}
74	26	7.946×10^9	6.045×10^{11}
80	28	1.014×10^{11}	1.237×10^{13}
88	27	5.231×10^{10}	1.246×10^{14}
90	27	1.322×10^{10}	8.592×10^{13}
100	31	9.195×10^{11}	1.007×10^{17}
223	32	5.747×10^{12}	4.685×10^{16}
236	30	1.238×10^{13}	1.510×10^{15}
256	31	2.445×10^{14}	
260	31	7.323×10^{12}	2.990×10^{15}
266	27	2.076×10^{11}	3.122×10^{14}
270	27	1.192×10^{15}	
272	30	3.212×10^{12}	2.481×10^{15}
293	29	3.242×10^{11}	2.827×10^{15}
348	29	2.478×10^{11}	1.914×10^{14}
352	27	4.230×10^{10}	3.154×10^{12}
387	27	6.322×10^{10}	6.790×10^{12}
521	28	4.518×10^{10}	6.914×10^{12}
527	26	9.913×10^9	9.746×10^{13}
762	27	2.174×10^{11}	5.707×10^{13}
798	26	1.672×10^{10}	2.515×10^{13}
810	26	8.596×10^{13}	
553	27	1.057×10^{10}	5.014×10^{13}
812	28	4.119×10^{11}	3.134×10^{13}
840	26	2.942×10^{10}	9.169×10^{12}
985	28	6.609×10^{10}	1.495×10^{14}
1000	26	2.510×10^{10}	3.772×10^{13}

TABLE III: Approximation of the number of FRST for a given polytope by the product of the FRT on each facet. When there are more than 21 lattice points in a facet, we apply the estimate of the number of FRT for that facet that are shown in Table II.

Fix a reflexive polytope. If a triangulation $\mathcal{T}_1$ can be brought to another triangulation $\mathcal{T}_2$ by a $GL(3,\mathbb{R})$ transformation of the lattice, $\mathcal{T}_1$ is equivalent to $\mathcal{T}_2$, and therefore the associated toric varieties are identical, leading to an overcounting. This effect will be most severe for those polytopes that give rise to the largest number of bases, which occur for large $h^{11}(B)$. Since there are only 38 polytopes with $h^{11}(B) \geq 26$, and these should account for the vast majority of bases, we study potential overcounting in these examples on a case by case basis. Note that if the facets have different numbers of lattice points then the FRT or FT of them can never be equivalent. For these reason, the 8 polytopes out of the 38

P	Cut-down by	P	Cut-down by
2	4!	4	$2! \times 2!$
8	3!	10	2!
12	2!	74	2!
80	2!	88	1!
128	$3! \times 2!$	130	2!
134	4!	136	$2! \times 2!$
223	2!	236	3!
256	4!	260	2!
266	2!	270	$2! \times 2!$
272	2!	293	2!
296	2!	348	2!
352	2!	387	$3! \times 2!$
521	1	553	2!
762	2!	780	2!
810	2!	812	2!

TABLE IV: Cutting-down coefficients.

that have indices $18, 90, 100, 527, 798, 840, 985, 1000$ are free from overcounting.

If there are K facets that can be brought to each other by a $GL(3,\mathbb{R})$ transformation then the our estimate could be cut down by at most a factor $K!$. This is because, for all the remaining cases with a set A_S of K facets of the same number of lattice points, these facets can be transformed into a configuration that they are symmetric about a plane H_p by an $SL(3,\mathbb{R})$ action which can be realized by applying several shear transformations successively. Therefore a triangulation of a facet in A_S can be taken to be equivalent to some triangulation of another facet in A_S by an $SL(3,\mathbb{R})$ transformation followed by a reflection about H_p together with a suitable transformation of the facets not in A_S. This leads to a cut-down by a factor $K!$ if such a transformation of the facets that are not in A_S always exists, and therefore $K!$ is the maximum cut-down factor. The result is summarized in Table IV. From these results it can be seen that automorphisms induce a reduction by at most a factor of 24. After cutting down, the estimate for lower and upper bounds on the number of FRST for $h^{11}(B) \geq 26$ polytopes is given in Table V.

Taking these cut-downs into consideration and the fact that the numbers different bases for $h^{11}(B) \geq 26$ are much larger than those for $h^{11}(B) \leq 25$, their number of FRST provides a good estimate of the total number of base spaces. Using those upper and lower bounds, we estimate that

$$5.780 \times 10^{14} \lesssim N_{\text{bases}} \lesssim 1.831 \times 10^{17}. \tag{4}$$

Mathematically, this is an estimate on the number of smooth weak Fano toric threefolds.

3. The Cost of Seven-brane Gauge Symmetry

In this section we study the cost of tuning all gauge groups in Table VI on seven-branes wrapped on any toric divisor in any smooth weak Fano toric threefold.

h_{11}	P	Lower bound	Upper bound
26	4	3.188×10^{11}	
26	18	2.899×10^{9}	4.436×10^{11}
26	74	3.973×10^{9}	2.023×10^{11}
26	128	3.217×10^{11}	
26	134	7.538×10^{10}	
26	136	6.933×10^{11}	
26	296	1.120×10^{11}	
26	527	9.913×10^{9}	9.746×10^{13}
26	780	7.540×10^{11}	
26	798	1.672×10^{10}	2.515×10^{13}
26	810	4.298×10^{13}	
26	840	2.942×10^{10}	9.169×10^{12}
26	1000	2.510×10^{10}	3.772×10^{13}
27	88	5.231×10^{10}	1.246×10^{14}
27	90	1.322×10^{10}	8.592×10^{13}
27	130	5.87×10^{12}	
27	266	1.038×10^{11}	1.561×10^{14}
27	270	2.980×10^{14}	
27	352	2.115×10^{10}	1.577×10^{12}
27	387	5.268×10^{9}	5.658×10^{11}
27	553	5.285×10^{9}	2.507×10^{13}
27	762	1.087×10^{11}	2.854×10^{13}
28	80	5.070×10^{10}	6.185×10^{12}
28	521	2.259×10^{10}	3.457×10^{12}
28	812	2.060×10^{11}	1.567×13^{13}
28	985	6.609×10^{10}	1.495×10^{14}
29	293	1.621×10^{11}	1.414×10^{15}
29	348	1.239×10^{11}	9.570×10^{13}
30	236	2.063×10^{12}	2.517×10^{14}
30	272	1.606×10^{12}	1.241×10^{15}
31	2	1.264×10^{14}	
31	10	2.855×10^{12}	7.290×10^{14}
31	100	9.195×10^{11}	1.007×10^{17}
31	256	1.019×10^{13}	
31	260	3.662×10^{12}	1.495×10^{15}
32	223	2.874×10^{12}	2.343×10^{16}
35	8	3.867×10^{13}	2.828×10^{16}
35	12	3.858×10^{13}	2.425×10^{16}

TABLE V: Approximation of the number of FRST for the polytope by the product of the FRT on each facet after a proper cut-down.

Recall from the introduction that geometric gauge symmetry on seven-branes in F-theory can be encoded in the structure of a Calabi-Yau elliptic fibration X. Let $X \xrightarrow{\pi} B$ be this elliptic fibration with base B given in Weierstrass form

$$y^2 = x^3 + fx + g, \tag{5}$$

with associated discriminant locus

$$\Delta = 4f^3 + 27g^2 = 0, \tag{6}$$

where $f \in \mathcal{O}(-4K_B)$, $g \in \mathcal{O}(-6K_B)$, and K_B is the canonical bundle of B. For generic $p \in B$, $\pi^{-1}(p)$ is a smooth elliptic curve, and for a generic p in $\Delta = 0$,

$\pi^{-1}(p)$ is one of the singular fibers classified by Kodaira. The set of Kodaira we consider is listed in Table VI. The Kodaira fiber of a particular component of the discriminant locus may be determined from the order of vanishing of f, g, and Δ along that component, and together with some additional data (see the appendix for details) this determines the gauge symmetry of the seven-brane on that component.

Fiber F	Gauge group G_F
I_2	$SU(2)$
I_{3ns}	$Sp(1)$
I_{3s}	$SU(3)$
I_{4ns}	$Sp(2)$
I_{4s}	$SU(4)$
I_{5ns}	$Sp(2)$
I_{5s}	$SU(5)$
I^*_{1ns}	$SO(9)$
I^*_{1s}	$SO(10)$
II	–
III	$SU(2)$
IV_{ns}	$Sp(1)$
IV_s	$SU(3)$
I^*_{0ns}	G_2
$I^*_{0s_1}$	$SO(7)$
$I^*_{0s_2}$	$SO(8)$
IV^*_{ns}	F_4
IV^*_s	E_6
III^*	E_7
II^*	E_8

TABLE VI: The set of Kodaira's singular fibers that we study, together with a label denoting whether or not they are split, and the associated gauge group.

The bases B that we study, as discussed in the last section, are smooth weak Fano toric threefolds. The general seven-brane configuration for such bases is one recombined seven-brane that does not carry non-abelian gauge symmetry; mathematically, this means that at a generic point in the complex structure moduli space of $X \to B$, for any such B, the variety $\Delta = 0$ is irreducible.

Obtaining non-abelian gauge symmetry, then, *requires* tuning in the complex structure of X by tuning f and g such that $\Delta = 0$ becomes reducible

$$\Delta = \prod_i \Delta_i, \tag{7}$$

where each component $\Delta_i = 0$ is a seven-brane that may carry a different gauge symmetry according to the orders of vanishing of f, g and Δ. A small deformation away from this sublocus in $\mathcal{M}_{cs}(X)$ with symmetry gives a small Higgsing of the associated gauge theory, the massive W-bosons of which are string junctions [32, 33] which can be systematically studied [34–36] in the geometry.

Our goal is to measure the cost of this tuning by computing the number of moduli that must be turned off in order to engineer Kodaira fibers of certain types on certain divisors. Specifically, we perform these computations for every Kodaira fiber in Table VI, for every toric divisor in every smooth weak Fano toric threefold. This computation is equivalent to computing the codimension in $\mathcal{M}_{cs}(X)$ on which a given Kodaira fiber type exists along a given divisor.

These computations are carried out as follows. Fix a three-dimensional reflexive polytope that contains integral points $v_i \in \mathbb{Z}^3$, where i is the index of the integral points. Let P_n be the polytope whose points are in one-to-one correspondence with global sections of $\mathcal{O}(-nK_B)$; it is defined by

$$P_n = \{m \in \mathbb{Z}^3 \,|\, m \cdot v_i + n \geq 0 \ \ \forall i\}. \tag{8}$$

To any $m \in P_n$ there is a monomial $\prod_i x_i^{m\cdot v_i + n}$ that has non-negative exponents by construction, and by this correspondence we will henceforth refer to such a monomial as a monomial in P_n. In the cases $n = 4, 6$ these monomials are the ones that may appear in f, g respectively, and if one constructs the most general f and g (that is, turns on all monomials) then $\Delta = 0$ is irreducible and there is no gauge symmetry on seven-branes.

Suppose we would like to compute how many monomials must be turned off in order to engineer a Kodaira fiber F and associated seven-brane gauge symmetry along along a given toric divisor $D_i := \{x_i = 0\}$. This can be done by sorting the monomials in P_n according to the exponents (orders of vanishing) of x_i. Then, using the data computed in the appendix and this sorting, it is straightforward to determine which monomials must be turned off or back on in order to engineer a given Kodaira fiber. Suppose N_{off} monomials are turned off and N_{on} are turned on; it is always the case that $N_{\text{off}} > N_{\text{on}}$. Then, obtaining a Kodaira fiber of type F on D_i requires tuning $N_{\text{off}} - N_{\text{on}}$ moduli, i.e. this gauge symmetry on a seven-brane on $x_i = 0$ occurs on a sublocus of codimension $N_{\text{off}} - N_{\text{on}}$ in $\mathcal{M}_{cs}(X)$.

For example, consider the case of a seven-brane on D_i with Kodaira fiber I_2, which corresponds to $SU(2)$ gauge symmetry and is the F-theory lift of two coincident $D7$-branes. From the appendix, we see this occurs when

$$f_0 = -3a_{20}^2, \ \ g_0 = 2a_{20}^2, \ \ g_1 = a_{20} f_1, \tag{9}$$

where $f_k \in \mathcal{O}(-4K_{D_i} + (4-k)N_{D_i|B})$, $g_k \in \mathcal{O}(-6K_{D_i} + (6-k)N_{D_i|B})$ and $a_{2k} \in \mathcal{O}(-2K_{D_i} + (2-k)N_{D_i|B})$. To engineer this form, the sections to be turned off are f_0, g_0 and g_1 while a_{20} is to be turned on. To do so algorithmically, we construct P_4, P_6 and P_2 whose points are monomials in the most general f, g and a_2. The subscript k in f_k, g_k and a_{2k} indicates the exponents of x_i in the monomials of the corresponding sections. In particular, in this case we need to find the points in P_4 that correspond to monomials that vanish to order 0, the points in P_6 that correspond to monomials vanish to order 0 and 1 and the points in P_2 that correspond to

monomials vanish to order 0, all with respect to x_i. The sum of the numbers of such points in P_4 and P_6 is N_{off} while the number of such points in P_2 is N_{on} since in order to tune I_2 on D_i, all the f_0, g_0 and g_1 monomials have to be turned off except those of the form given by Equation 9.

In this way, the cost of tuning a particular Kodaira fiber F and associated gauge symmetry G_F on a toric divisor D_i is $N_{\text{off}} - N_{\text{on}}$, where N_{off} and N_{on} are computed in accordance with the sections that must be tuned in order to achieve F on D_i. We denote the cost of symmetry of tuning such F on D_i with associated $3d$ reflexive polytope P as $C(P, D_i, F)$. From this data we compute various statistics.

We turn first to Figure 4, which is the plot of the unweighted average costs of tunings as a function of $h^{11}(B)$. Let $S(h^{11}(B))$ be the set of $3d$ reflexive polytopes with $h^{11}(B) + 4$ integral points, where the origin is included in the set of integral points. Each line in the figure is a function of $h^{11}(B)$ and F, and the associated unweighted average cost of symmetry for all toric divisors for all polytopes in $S(h^{11}(B))$ is

$$\frac{1}{|S(h^{11}(B))|} \sum_{P \in S(h^{11}(B))} \sum_{D_i \in P} \frac{C(P, D_i, F)}{h^{11}(B) + 3}. \qquad (10)$$

By unweighted, we mean that all polytopes are treated equally, without taking into account the fact that they have different numbers of FRST, and therefore different numbers of associated bases.

There are two things that can be immediately read off from Figure 4: 1) The unweighted average costs of tunings decreases sharply as $h^{11}(B)$ increases, although there is small fluctuation at the right end of the plot; 2) In general a gauge group of a higher rank requires more tunings than those of a lower rank. In particular, II^* costs the most while II costs the least. The first point is due to the observation that a polytope with higher $h^{11}(B)$ usually leads to polytopes P_n with less lattice points, hence less monomials. The second point can be understood by noting that tuning a gauge group of a higher rank usually involves turning off more monomials in P_4 and P_6, which dominates the overall costs since the monomials that are to be turned on live in P_2, which has much less lattice points than P_4 and P_6. The reason we present the unweighted plot here is that it gives a good approximation to the weighted plot, but can be understood by simple arguments. Those arguments can be made in the absence of the weighting process "perturbing" the averaging, so that only the numbers of monomials involved and the size of the polytopes P_n matter.

[1] Shaded area indicates there are no varieties with $h^{11}(B) = 32, 33$.

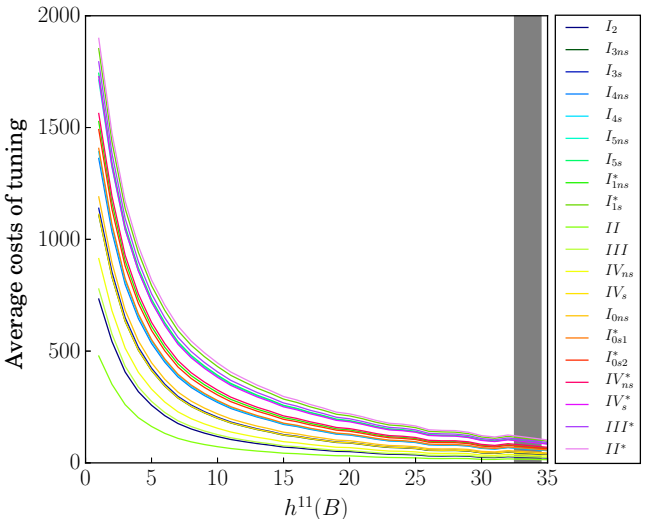

FIG. 4: Costs of unweighted tunings[1].

For fixed F and G_F, Table VII lists the maximal and minimal values of $C(P, D_i, F)$ for any toric divisors of a smooth weak Fano toric threefold. Note that, contrary to common expectations, the maximal tunings do not occur for $B = \mathbb{P}^3$ but instead for B that are associated to FRST of polytopes 7 and 11. Note also that though the average weighted costs of tuning in Figure 5 is always at least $O(20)$, Table VII shows that there do exist divisors where obtaining non-abelian gauge symmetry only requires tuning a handful of moduli, for example a minimum of 2 in the case of $SU(2)$.

The plot of weighted average tuning costs is shown in Figure 5, where the weighting takes into account the estimated number of FRST per $3d$ reflexive polytope. For fixed $h^{11}(B)$ and F, this weighted average is defined by

$$\sum_{P \in S(h^{11}(B))} \frac{N_P}{\sum_{P' \in S(h^{11}(B))} N_{P'}} \sum_{D_i \in P} \frac{C(P, D_i, F)}{h^{11}(B) + 3}. \qquad (11)$$

Here the method of estimating the number of FRST N_P depends on the value of $h^{11}(B)$. Recall from the previous section that for $h^{11}(B) \leq 10$, N_P is the exact number of FRST of P. When $11 \leq h^{11}(B) \leq 22$ we apply method B to estimate N_P, and when $23 \leq h^{11}(B) \leq 25$ we apply method C. Since applying method C will assign the same N_P to each P, in this region the weighted costs are numerically equivalent to the unweighted costs. When $h^{11}(B) \geq 26$ we take N_P to be the average of the lower bound and the upper bound given by method D.

Quite surprisingly, comparing Figures 4 and 5 we see the weighting does not significantly change the behavior of the costs of the tunings as a function of $h^{11}(B)$. The curves fluctuate a bit more in region D but in regions A and B, where the numbers of FRST of the polytopes are computed exactly or estimated more

Fiber	Maximum	Polytope	Minimum	Polytope	Gauge group
I_2	1532	7, 11	2	8, 10, 16, 29, 35, 58, 88, 156, 178, 256, 258, 260, 387, 549, 670, 1462	$SU(2)$
I_{3ns}	2226	7, 11	6	8, 10	$Sp(1)$
I_{3s}	2289	7, 11	6	8, 10	$SU(3)$
I_{4ns}	2632	7, 11	10	8	$Sp(2)$
I_{4s}	2695	7, 11	10	8	$SU(4)$
I_{5ns}	3147	7, 11	24	8	$Sp(2)$
I_{5s}	3210	7, 11	24	8	$SU(5)$
I^*_{1ns}	2913	7, 11	15	8	$SO(9)$
I^*_{1s}	3364	7, 11	28	8	$SO(10)$
III	1623	7, 11	3	8, 10, 16, 29, 35, 58, 88, 156, 178, 256, 258, 260, 387, 549, 670, 1462	$SU(2)$
IV_{ns}	1876	7, 11	4	8, 10, 16, 29, 35, 58, 88, 156, 178, 256, 258, 260, 387, 549, 670, 1462	$Sp(1)$
IV_s	2236	7, 11	7	8, 10	$SU(3)$
I^*_{0ns}	2372	7, 11	8	8	G_2
$I^*_{0s_1}$	2723	7, 11	11	8	$SO(7)$
$I^*_{0s_2}$	2858	7, 11	14	8	$SO(8)$
IV^*_{ns}	2968	7, 11	16	8	F_4
IV^*_s	3202	7, 11	22	8	E_6
III^*	3293	7, 11	26	8	E_7
II^*	3429	7, 11	30	8	E_8

TABLE VII: Maximal and minimal costs of tuning for each fiber type and associated gauge group. Listed are the maximum and minimum values of $C(P, D_i, F)$ for given fibers and polytopes. Divisor index data is omitted in this plot.

accurately, the percent difference between unweighted and weighted averages are no more than 16%. The maximal percent difference between the weighted and unweighted averages in any region is 21.5%. In regions A, B and C the cutting-down factor is not taken into consideration since a thorough investigation in these regions is very time consuming and the large number of polytopes for lower $h^{11}(B)$ likely leads to an average cancellation effect.

Our calculations show that tuning a fixed fiber type on a divisor D_{vert} corresponding to a vertex of a $3d$ reflexive polytope P usually costs more than on D_{int} corresponding to a non-vertex lattice point of P. The average difference between the unweighted costs of tuning on D_{vert} and D_{int} is shown in Figure 6. Note that there are no non-vertex lattice points in P when $h^{11}(B) = 1$, hence there is no such difference. The ratio between average costs of tuning on D_{vert} and D_{int} is shown in Figure 7.

A question naturally arises when we consider the Equation 8. Because of the linearity of this equation, it happens that tuning a gauge group on a divisor D_1 corresponding to v_1 may lead to tuning another gauge group on divisor D_2 corresponding to v_2. That happens when the monomials that are tuned to obtain a gauge group on D_2 is a subset of the monomials tuned to obtain a gauge group on D_1. A direct calculation shows that this never occurs when tuning fiber types I_2, I_3, I_4 and I_5. This can happen when tuning other fiber types,but any tuning on D_1 never forces the monomials f and g to vanish to order 4 and 6 on any other divisor respectively In one case that we have studied in depth, tuning E_7 on a divisor can lead to tuning other gauge groups on divisors that are adjacent in some triangulations, but it never occurs that a higher rank gauge group arises in this process or it leads to f and g monomials that vanish to order 4 and 6 respectively on another divisor.

4. Discussion

In this work we study the costs of tuning gauge groups on seven-branes in F-theory, where the seven-brane is wrapped on any toric divisor in any smooth weak Fano toric threefold. These may be constructed from FRST of 3d reflexive polytopes that are classified by Kreuzer and Skarke. A proper calculation of the weighted average costs requires an estimate of the numbers of FRST of the polytopes. The numbers of FRST of the polytopes with higher $h^{11}(B)$ dominate the number of base spaces so that an estimate of the numbers of FRST of those polytopes gives us an estimate of the total number of bases, $5.8 \times 10^{14} \lesssim N_{\text{bases}} \lesssim 1.8 \times 10^{17}$. Thus, we study about one quadrillion F-theory compactifications.

We investigate the polytopes P_n in the dual lattice, whose points correspond to the sections of $\mathcal{O}(-nK_B)$ which can be turned off or on in order to tune a gauge group on a seven-brane on a divisor D_i. The sections involved are determined by the fiber type and can be sorted by their orders of vanishing along D_i. The exact numbers of the sections must be turned off and turned on to engineer gauge symmetry can be calculated accordingly for each base space. This determines the codimension of the sublocus in $\mathcal{M}_{cs}(X)$ on which seven-brane gauge symmetry exists on D_i; this is the cost of symmetry.

Both the unweighted and weighted average costs of symmetry are given in the paper. They are calculated according to Equation 10 and Equation 11 respectively,

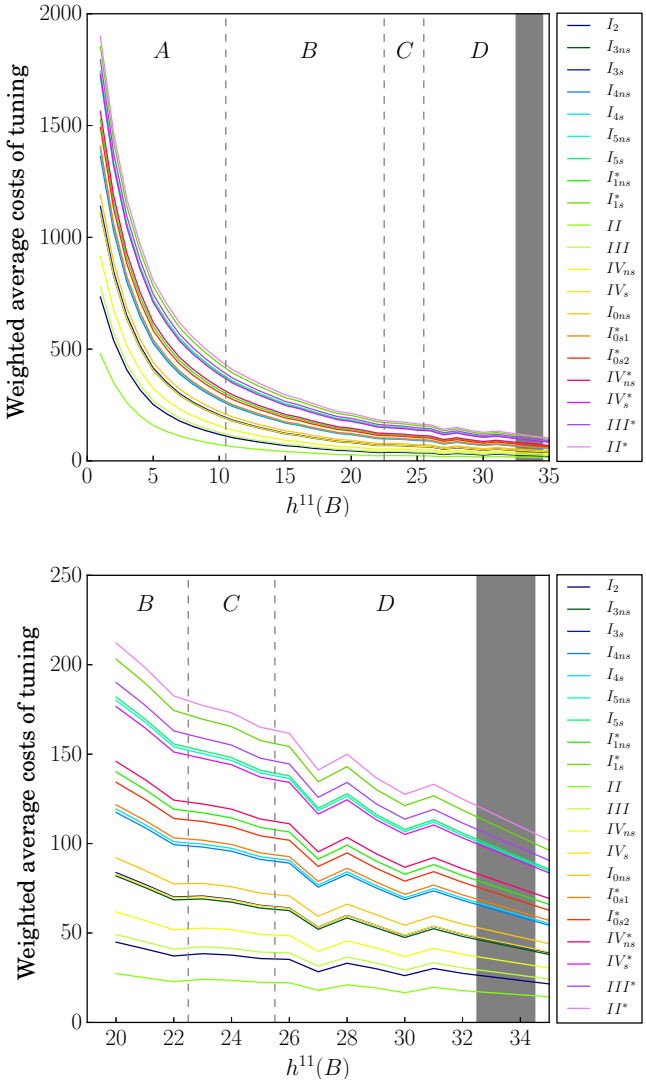

FIG. 5: Average costs of tunings after weighting by the numbers of FRST of the polytopes. The plot is divided into 4 regions. The labels A, B, C and D denotes the different methods we apply in the corresponding regions to get the numbers of FRST of the polytopes in the weighting process. *Top:* Weighted average costs for all $h^{11}(B)$. *Bottom:* Focusing on the region $h^{11}(B) \geq 20$.

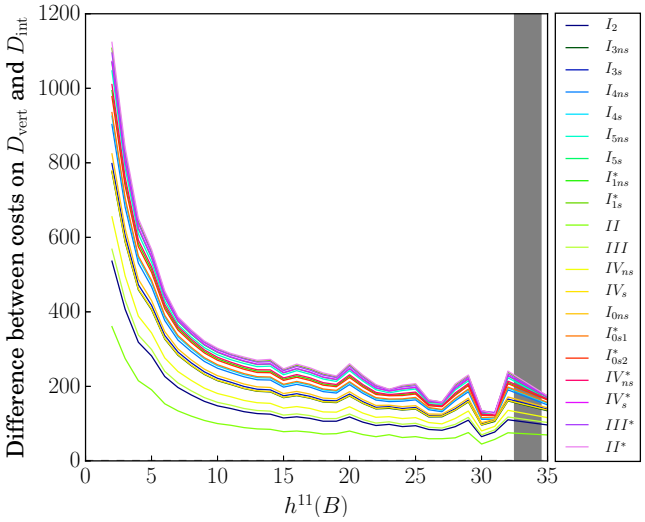

FIG. 6: Average difference between costs of tuning on $D_{\rm vert}$ and $D_{\rm int}$

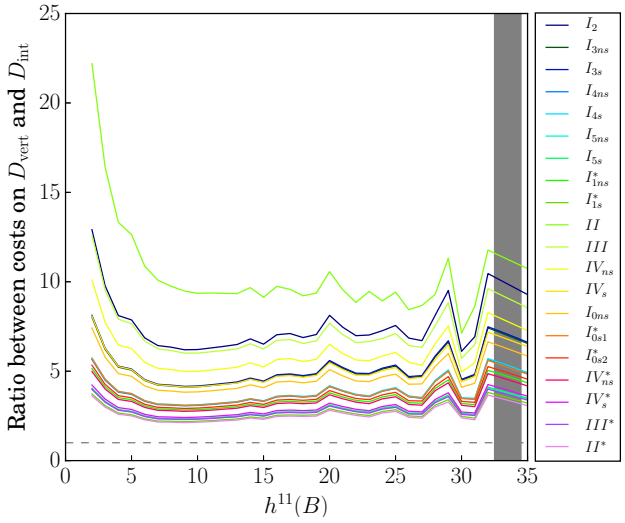

FIG. 7: Ratio between costs of tuning on $D_{\rm vert}$ and $D_{\rm int}$. The dashed line in the plot denotes $y = 1$ which shows that the costs of tuning on $D_{\rm vert}$ are always larger than those on $D_{\rm int}$.

where our estimates of the number of FRST of the polytopes is applied in the weighting process. We find that both the unweighted costs and weighted costs drop steeply as $h^{11}(B)$ increases. When $h^{11}(B) \leq 5$ the average symmetry costs range from $O(250)$ to $O(2000)$; when $h^{11}(B) \geq 10$ they drop down below $O(500)$; and when $h^{11}(B) > 20$ they range from $O(25)$ to $O(200)$.

We find that the costs of tuning of the gauge groups depend significantly on the specific divisor on which symmetry is to be tuned. There exist divisors in certain polytopes on which only a few moduli need to be tuned to achieve symmetry, while there also exist divisors in certain polytopes where a few thousands moduli need to be tuned. The average costs as a function of $h^{11}(B)$ are plotted in Figures 4 and 5. We also show that cost of symmetry depends on the type of divisor. Specifically, tuning symmetry on divisors that correspond to a vertex of the 3d reflexive polytope costs more than tuning on the divisors that correspond to the interior points.

In summary, our study of F-theory compactifications without non-Higgsable clusters shows that when non-abelian gauge symmetry must be tuned, it typically occurs on subloci in $\mathcal{M}_{cs}(X)$ of codimension $O(25)$-$O(250)$.

While this cost of symmetry is less severe than in the work of [28], it still represents a significant cosmological challenge. We believe this result further motivates the study of moduli stabilization on special subloci in moduli space, and also the study of non-Higgsable clusters.

Acknowledgements. We would like to thank Ross Altman, Andreas Braun, Jonathan Carifio, Cody Long, Brent Nelson, Ben Sung, and Washington Taylor for discussions about this work. JH is supported by NSF Grant PHY-1620526 and startup funding from Northeastern University. He thanks the Center for Theoretical Physics at MIT for hospitality at various stages of this work. This work was performed in part at the Aspen Center for Physics, which is supported by National Science Foundation grant PHY-1066293.

APPENDIX

Let $X \xrightarrow{\pi} B$ be an elliptic fibration in Weierstrass form, where $y^2 = x^3 + fx + g$ with $f \in \mathcal{O}(-4K_B)$ and $g \in \mathcal{O}(-6K_B)$, which has a discriminant locus $\Delta = 4f^3 + 27g^2$. We will consider the tuning of gauge symmetry on a divisor Z defined locally by $z = 0$; in toric cases, z will be a homogeneous coordinate and therefore Z a toric divisor. This allows us to expand f and g as $f = f_0 + f_1 z + f_2 z^2 + f_3 z^3 + \dots$ and $g = g_0 + g_1 z + g_2 z^2 + g_3 z^3 + \dots$, where $f_i \in \mathcal{O}(-4K_Z + (4-i)N_{Z|B})$ and $g_i \in \mathcal{O}(-6K_Z + (6-i)N_{Z|B})$. We will also utilize $a_{ni} \in \mathcal{O}(-nK_Z + (n-i)N_{Z|B})$, which will be relevant in studying tuning. Since we are only interested in the structure of gauge groups, we will only consider codimension one singularities. Throughout we use "node" to mean the node of a Dynkin diagram, represented geometrically by a $\mathbb{P}^1$ fiber. Relevant arguments of the conditions under which the intersection diagrams of the nodes are the duals of the Dynkin diagrams of the gauge groups can be found in [26, 37].

We are now ready to investigate the singularities of the elliptic fibration. We will study the relationship between sections the ensures the existence of each fiber type, and in some cases we will resolve the codimension one singularities to study their structure. We denote resolutions by notation of the form $X \xleftarrow{(x_1,x_2,\dots|e)} X'$ where the resolution is performed along $\cap_i\{x_i = 0\}$ and $e = 0$ is the exceptional divisor; this gives replacements $x_i \mapsto ex_i$. The required tunings are summarized in Table VIII.

$\mathbf{I_1}$. If X is smooth, then Δ has generic Kodaira fiber I_1. An I_1 fiber along Z can be obtained by $f_0 = -3a_{20}^2$ and $g = 2a_{20}^3$. X is smooth.

$\mathbf{I_2}$. Let $f_0 = -3a_{20}^2, g = 2a_{20}^3, g_1 = -a_{20}f_1$. There is one singularity at $x = a_{20}, y = 0, z = 0$. Shift the singularity to $(0,0,0)$ by redefining x and do the blow up $X \xleftarrow{(x,y,z|e)} X'$. There are no more codimension 1 singularities after the blow-up. The exceptional divisor e_0 is fibered by genus 0 curves in the new $\mathbb{P}^2$ associated with the blow-up. This gives us $G = SU(2)$.

$\mathbf{I_3}$. Let $f_0 = -3a_{20}^2, g_0 = 2a_{20}^3, g_1 = -a_{20}f_1, f_1 = a_{20}a_{21}, g_2 = \frac{a_{20}}{12}(a_{21}^2 - 12f_2)$. There is one singularity at $x = a_{20}, y = 0, z = 0$. Shift it to $(0,0,0)$ and do the blow up $X \xleftarrow{(x,y,z|e)} X'$. There are no more codimension 1 singularities after the blow-up. An analysis of X' shows that $e = 0$ is fibered by two lines that swap under encircling $a_{20} = 0$ if and only if a_{20} is not a perfect square. Thus, if a_{20} is a perfect square, $G = SU(3)$; if it is not, $G = Sp(1) = SU(2)$.

$\mathbf{I_4}$. Let $f_0 = -3a_{20}^2, g = 2a_{20}^3, g_1 = -a_{20}f_1, f_1 = a_{20}a_{21}, g_2 = \frac{a_{20}}{12}(a_{21}^2 - 12f_2), g_3 = \frac{1}{216}(a_{21}^3 + 36a_{21}f_2 - 216f_3)$. Again we shift the singularity to $(0,0,0)$ and do the blow-up $X \xleftarrow{(x,y,z|e_1)} X'$. The resulting variety is still singular. The singular locus is along $e_1 = 0, x = -\frac{a_{21}z}{6}, y = 0$ so we shift it to $(0,0,0)$ and do a second blow up $X' \xleftarrow{(x,y,e_1|e_2)} X''$. There are no more codimension 1 singularities after the blow-up. The fiber of $e_1 = 0$ splits into two lines that swap upon encircling $a_{20} = 0$ if and only if a_{20} is not a perfect square. Henceforth by "split" we will mean that two nodes do not swap under encircling some locus, here $a_{20} = 0$. A further analysis of X'' fibers shows that $G = SU(4)$ if a_{20} is a perfect square then $G = SU(4)$; if not, then $G = Sp(2)$.

$\mathbf{I_5}$. Let $f_0 = -3a_{20}^2, g = 2a_{20}^3, g_1 = -a_{20}f_1, f_1 = a_{20}a_{21}, g_2 = \frac{a_{20}}{12}(a_{21}^2 - 12f_2), g_3 = \frac{1}{216}(a_{21}^3 + 36a_{21}f_2 - 216f_3), g4 = -a_{20}f_4 + \frac{a_{21}f_3}{6}, f_2 = -\frac{a_{21}^2}{12}$. The first blow-up along the shifted singularity is again $X \xleftarrow{(x,y,z|e_1)} X'$. The second blow-up along the shifted singularity is $X' \xleftarrow{(x,y,e_1|e_2)} X''$. There are no more codimension 1 singularities after the blow-up. The fibers of $e_1 = 0$ give the exterior nodes on the A_4 Dynkin diagram, and the fibers of $e_2 = 0$ give the interior nodes. The exterior nodes split if and only if a_{20} is a perfect square, as do the interior nodes. Thus if a_{20} is a perfect square, $G = SU(5)$; if not, $G = Sp(2)$.

$\mathbf{I_1^*}$. For I_1^* f series starts with f_2 term whereas g series starts with g_3 terms. Let $f_2 = -3a_{21}^2, g_3 = 2a_{21}^3$. Blow up the singularity at $(0,0,0)$ by $X \xleftarrow{(x,y,z|e_1)} X'$. Two singular loci appear after this blow-up. We shift the variety to make one of the singularities sit at $x = 0, y = 0, e_1 = 0$ then blow it up by $X' \xleftarrow{(x,y,e_1|e_2)} X''$. Two singular locus appear after this blow up and one of them is at $e_1 = 0, e_2 = 0, y = 0$ and we blow it up by $X'' \xleftarrow{(e_1,e_2,y|e_3)} X'''$. We are left with one singularity after this blow-up and this singularity is given by an algebraic equation of the form $e_2 A = yB$. After a small resolution $X''' \xleftarrow{(e_1,y|e_4)} X''''$ there are no more codimension 1 singularities. There are four divisors when

we go into the exceptional locus. We check the case when they split. The split condition is given by letting $f_3 = c_1 a_{21} a_{11}^2, g_4 = c_2 a_{21}^2 a_{11}^2$, c_1, c_2 are two arbitrary numbers. Non-split case gives us $SO(9)$ and split case gives us $SO(10)$.

II. Tune f_0 and g_0 to zero to get a type II fiber. This has no gauge algebra.

III. Tune f_0, g_0 and g_1 to zero. X is singular and we blow it up by $X \xleftarrow{(x,y,z|e_1)} X'$. There are no more codimension 1 singularities after the blow-up. The exceptional divisor is fibered by a genus 0 curve which gives us $SU(2)$.

IV. Tune f_0, f_1, g_0, and g_1 to zero. There is a singularity in the fibration and we blow it up by $X \xleftarrow{(x,y,z|e_1)} X'$. There are no more codimension 1 singularities after the blow-up. The fiber of the exceptional divisor splits when g_2 is a perfect square, $g_2 = a_{31}^2$. In that case $G = SU(3)$; if g_2 is not a perfect square, $G = Sp(1)$.

$\mathbf{I_0^*}$. Let $f = f_2 z^2, g = g_3 z^3$. First we do $X \xleftarrow{(x,y,z|e_1)} X'$. The resulting variety has the form $y^2 = e_1 P$ in the ambient space so that we can do a small resolution $X' \xleftarrow{(e_1,y|e_2)}$. The resulting variety, without any codimension 1 singularities, when it splits, gives 4 four nodes. The splitting is given by the relationship $f_2 = -a_{21}^2 - a_{21} a_{21}' - a_{21}'^2, g_3 = a_{21}^2 a_{21}' + a_{21} a_{21}'^2$. Let's call the node given by $e_1 = 0$ N_1 and by $e_2 = 0$ $N_{21}, N_{22}.N_{23}$. N_1 intersects with N_{21} N_{22} and N_{23} at 3 different points. There are no other intersections. This gives us $SO(8)$. There are two different situations if I_0^* does not fully split. When f_2 and g_3 are two generic sections, there are 2 nodes given by $e_1 = 0$ and $e_2 = 0$, call them N_1 and N_2 respectively. N_1 is fibered by $\mathbb{P}^1$ and N_2 is fibered by 3 $\mathbb{P}^1$'s. The 3 $\mathbb{P}^1$'s in N_2 are getting mapped to each other when encircling $e_2 = 0$. The intersection diagram gives us G_2. When $f_2 = a_{42} - a_{21}^2, g_3 = -a_{42} a_{21}$, two of the three nodes N_{21} N_{22} N_{23}, say N_{22} and N_{23}, when encircling $e_2 = 0$, get mapped to each other. This intersection diagram gives us $SO(7)$.

$\mathbf{IV}^*$. Let $f = f_3 z^3, g = g_4 z^4$. We need to do 4 blow-ups to resolve the singularities until there are no codimension 1 singularities. The exceptional locus split when $g_4 = a_{32}^2$, let's call the node given by $e_1 = 0$ N_1, by $e_2 = 0$ N_{21} and N_{22}, by $e_3 = 0$ N_{31} and N_{32} and by $e_4 = 0$ N_4. N_1 intersects with N_4, N_4 with N_{31} and N_{32} at two different points, N_{31} with N_{21} and N_{32} with N_{22}. There are no more intersections. This gives us E_6. When g_4 is a generic section, $e_2 = 0$and $e_3 = 0$ do not split. $N_2 1$ gets mapped to $N_2 2$ while encircling $e_2 = 0$ and $N_3 1$ to $N_3 2$ while encircling $e_3 = 0$. The intersection diagram gives us F_4.

$\mathbf{III}^*$. Let $f = f_3 z^3$, $g = g_5 z^5$. We do not perform the blowup explicitly, resolutions yield exceptional divisors that are fibered by genus 0 curves whose intersection diagram gives us E_7.

$\mathbf{II}^*$. Let $f = f_4 z^4$, $g = g_5 z^5$. We do not perform the blowup explicitly, resolutions yield exceptional divisors that are fibered by genus 0 curves whose intersection diagram gives us E_8.

Type	Tuned off	Tuned on	Gauge group
I_2	f_0 g_0 g_1	a_{20}	$SU(2)$
I_{3ns}	f_0 f_1 g_0 g_1 g_2	a_{20} a_{21}	$Sp(1)$
I_{3s}	f_0 f_1 g_0 g_1 g_2	a_{10} a_{21}	$SU(3)$
I_{4ns}	f_0 f_1 g_0 g_1 g_2 g_3	a_{20} a_{21}	$Sp(2)$
I_{4s}	f_0 f_1 g_0 g_1 g_2 g_3	a_{10} a_{21}	$SU(4)$
I_{5ns}	f_0 f_1 f_2 g_0 g_1 g_2 g_3 g_4	a_{20} a_{21}	$Sp(2)$
I_{5s}	f_0 f_1 f_2 g_0 g_1 g_2 g_3 g_4	a_{10} a_{21}	$SU(5)$
I_{1ns}^*	f_0 f_1 f_2 g_0 g_1 g_2 g_3	a_{21}	$SO(9)$
I_{1s}^*	f_0 f_1 f_2 f_3 g_0 g_1 g_2 g_3 g_4	a_{21} a_{11}	$SO(10)$
II	f_0 g_0	–	–
III	f_0 g_0 g_1	–	$SU(2)$
IV_{ns}	f_0 f_1 g_0 g_1	–	$Sp(1)$
IV_s	f_0 f_1 g_0 g_1 g_2	a_{31}	$SU(3)$
I_{0ns}^*	f_0 f_1 g_0 g_1 g_2	–	G_2
$I_{0s_1}^*$	f_0 f_1 f_2 g_0 g_1 g_2 g_3	a_{21} a_{42}	$SO(7)$
$I_{0s_2}^*$	f_0 f_1 f_2 g_0 g_1 g_2 g_3	a_{21} a_{21}'	$SO(8)$
IV_{ns}^*	f_0 f_1 f_2 g_0 g_1 g_2 g_3	–	F_4
IV_s^*	f_0 f_1 f_2 g_0 g_1 g_2 g_3 g_4	a_{32}	E_6
III^*	f_0 f_1 f_2 g_0 g_1 g_2 g_3 g_4	–	E_7
II^*	f_0 f_1 f_2 f_3 g_0 g_1 g_2 g_3 g_4	–	E_8

TABLE VIII: Sections needed to be tune off or on to get the required gauge group. $f_i \in \mathcal{O}(-4K_Z + (4-i)N_{Z|B}), g_i \in \mathcal{O}(-6K_Z + (6-i)N_{Z|B}), a_{ni} \in \mathcal{O}(-nK_Z + (n-i)N_{Z|B})$.

[1] L. Kofman, A. D. Linde, X. Liu, A. Maloney, L. McAllister, and E. Silverstein, JHEP **05**, 030 (2004), hep-th/0403001.

[2] A. Grassi, J. Halverson, J. Shaneson, and W. Taylor, JHEP **01**, 086 (2015), 1409.8295.

[3] C. Vafa, Nucl. Phys. **B469**, 403 (1996), hep-th/9602022.

[4] A. Sen, Nucl. Phys. **B475**, 562 (1996), hep-th/9605150.

[5] A. Sen, Phys. Rev. **D55**, 7345 (1997), hep-th/9702165.

[6] S. Kachru, R. Kallosh, A. D. Linde, and S. P. Trivedi, Phys. Rev. **D68**, 046005 (2003), hep-th/0301240.

[7] V. Balasubramanian, P. Berglund, J. P. Conlon, and F. Quevedo, JHEP **03**, 007 (2005), hep-th/0502058.

[8] D. R. Morrison and C. Vafa, Nuclear Phys. B **473, 476**, 74 (1996), ISSN 0550-3213.

[9] S. Ashok and M. R. Douglas, JHEP **01**, 060 (2004), hep-th/0307049.

[10] F. Denef and M. R. Douglas, JHEP **05**, 072 (2004), hep-th/0404116.

[11] F. Denef and M. R. Douglas, JHEP **03**, 061 (2005), hep-th/0411183.

[12] F. Denef and M. R. Douglas, Annals Phys. **322**, 1096 (2007), hep-th/0602072.

[13] K. Kodaira, Amer. J. Math. **86**, 751 (1964), ISSN 0002-9327.

[14] K. Kodaira, Amer. J. Math. **88**, 682 (1966), ISSN 0002-9327.

[15] K. Kodaira, Amer. J. Math. **90**, 55 (1968), ISSN 0002-9327.

[16] M. Bershadsky, K. A. Intriligator, S. Kachru, D. R. Morrison, V. Sadov, and C. Vafa, Nucl. Phys. **B481**, 215 (1996), hep-th/9605200.

[17] S. Cecotti, C. Cordova, J. J. Heckman, and C. Vafa, JHEP **07**, 030 (2011), 1010.5780.

[18] K. Dasgupta, G. Rajesh, and S. Sethi, JHEP **08**, 023 (1999), hep-th/9908088.

[19] D. R. Morrison and W. Taylor, Central Eur. J. Phys. **10**, 1072 (2012), 1201.1943.

[20] D. R. Morrison and W. Taylor, Fortsch. Phys. **60**, 1187 (2012), 1204.0283.

[21] J. Halverson (2016), 1603.01639.

[22] D. R. Morrison, D. S. Park, and W. Taylor (2016), 1610.06929.

[23] L. B. Anderson and W. Taylor, JHEP **08**, 025 (2014), 1405.2074.

[24] D. R. Morrison and W. Taylor, JHEP **05**, 080 (2015), 1412.6112.

[25] J. Halverson and W. Taylor, JHEP **09**, 086 (2015), 1506.03204.

[26] W. Taylor and Y.-N. Wang, JHEP **01**, 137 (2016), 1510.04978.

[27] J. Halverson, B. D. Nelson, and F. Ruehle (2016), 1609.02151.

[28] A. P. Braun and T. Watari, JHEP **01**, 047 (2015), 1408.6167.

[29] T. Watari, JHEP **11**, 065 (2015), 1506.08433.

[30] M. Kreuzer and H. Skarke, Adv. Theor. Math. Phys. **2**, 847 (1998), hep-th/9805190.

[31] V. Kaibel and G. M. Ziegler, ArXiv Mathematics e-prints (2002), math/0211268.

[32] M. R. Gaberdiel and B. Zwiebach, Nuclear Phys. B **518**, 151 (1998), ISSN 0550-3213, URL `http://dx.doi.org/10.1016/S0550-3213(97)00841-9`.

[33] O. DeWolfe and B. Zwiebach, Nuclear Phys. B **541**, 509 (1999), ISSN 0550-3213, URL `http://dx.doi.org/10.1016/S0550-3213(98)00743-3`.

[34] A. Grassi, J. Halverson, and J. L. Shaneson, J. High Energy Phys. pp. 1–47 (2013), `arXiv:1306.1832`.

[35] A. Grassi, J. Halverson, and J. L. Shaneson, Commun. Math. Phys. **336**, 1231 (2015), 1402.5962.

[36] A. Grassi, J. Halverson, and J. L. Shaneson (2014), 1410.6817.

[37] S. Katz, D. R. Morrison, S. Schafer-Nameki, and J. Sully, JHEP **08**, 094 (2011), 1106.3854.